ISSN 1392–1207. MECHANIKA. 2017 Volume 23(1): 153–159

Prediction of and experimental study on cutting force of austempered vermicular graphite cast iron using artificial neural network

Ahmet Mavi*, Semih Ozden, İhsan Korkut*****
**Gazi University, Technical Sciences Vocational College, Ankara, Turkey, E-mail: amavi@gazi.edu.tr*
***Gazi University, Technical Sciences Vocational College, Ankara, Turkey, E-mail: semihozden@gmail.com*
****Gazi University, Faculty of Technology, Ankara, Turkey, E-mail: ikorkut@gazi.edu.tr*

crossref http://dx.doi.org/10.5755/j01.mech.23.1.13699

1. Introduction

It is important that optimum cutting parameters must be defined to obtain desired surface quality and cutting force for all machining processes (surface milling, drilling, turning, etc.). It can be seen that cutting speed, cutting depth, feed rate, cutting tool angle, cutting type-material, and cutting geometry have significant effects on the cutting forces [1]. Cast irons are divided into several types parallel to the developments in technology and started to be used in every field of industry [2].

Vermicular graphite cast irons (VGCI) are widely used specially in the automotive industry. For this reason, it has become a hot topic among researchers. Different heat treatments are applied to improve mechanical properties of cast irons. Heat treatment which provides the highest toughness and strength is austempering [3-5]. The effects of austempering heat treatment are clearly seen in the studies on the spheroid graphite cast irons [6-8]. However, the austempering treatment of VGCI is very limited in the literature.

Machinability can be defined as the property of the material which governs the ease or difficulty with which it can be machined under a given set of conditions. In this way, the concept that a work material is more machinable than another signifies that it causes longer tool life, requires lesser cutting force and power, and provides better surface finish. Machinability is assessed in terms of machinability criteria and involves essentially minimizing the cost and maximizing the rate of production [9]. Choosing suitable machining variables is important to improve the machined cutting force, and further widen their application. In the workshop level, the machinists set the parameters based on their experience and trial-and-error approach, which induces the additional production cost and the expert requirement [10]. Therefore, some researchers developed a cutting force model based on a combination of different machining parameters to predict the work piece surface quality using machine learning methods. In these studies, different methods and materials have been studied and experimented.

Bartarya and Choudhury [11] developed a regression model for the finish machining of EN31 steel. The models show that the dependence of the cutting forces, i.e. cutting, radial, and axial forces, and surface roughness on machining parameters is significant; hence, they could be used for making predictions for the forces and surface roughness. Aouici et al. presents an experimental contribution that focuses on prediction and optimization of both surface roughness and cutting force components during hard turning of AISI H11 steel using the response surface methodology [12].

Irgolic et al. predicted the cutting forces of milling very hard materials, such as graded materials. The error in predicting cutting forces was smaller than 10%. This is a very reliable prediction for the planned cutting force, which allows us to operate the machine in a safe zone [13]. In a previous study [14], the cutting parameters were optimized using signal to noise ratio and the analysis of variance. The effects of cutting speed and feed rate on surface roughness, cutting force, and tool wear were analyzed. The results revealed that the feed rate was the most significant parameter influencing the surface roughness and cutting force.

In the present study, cutting force (*f*) resulting from the machinability of austempered vermicular graphite cast irons (VGCI) is considered as a measurable output parameter with respect to the input parameters, namely cutting speed, feed rate, and hardness. The objective of the present was to develop a mathematical modeling of machining processes in order to predict machining criteria. Polynomial regressions cannot always yield accurate modeling because the strong nonlinear nature of machining gives way to low correlation coefficients [9]. To determine the appropriate network structure, performance of the network consisting of a constant number of input and output layer neurons is measured with respect to changing numbers of the neurons in the two hidden layers, which are 3-15.

2. Testing procedures

2.1. Experimental setup and measurements

The material used in the present study is a vermicular graphite cast iron (VGCI). The chemical composition of the material is given in Table 1.

Table 1

Chemical composition of experimental VGCI (wt %)

C	Si	Mn	P	S	Cr	Cu	Mg	Sn	Ti
3.74	2.30	0.37	0.0027	0.014	0.0044	0.056	0.013	0.14	0.023

The length of the work piece bars was 270 mm with a 26 mm diameter. These specimens were austenitized at 900°C for 90 minutes and then rapidly transferred to a salt bath containing 50% KNO3 + 50% NaNO3, and each piece was kept in this bath at 320°C and 370°C for austempering for 60, 90, and 120 minutes to produce a different ausferrite structure morphology. The schematic diagram of the different heat treatment processes and experimental set up are shown in Fig. 1, a and b. Measured hardness values at different austempering times and temperatures are given in Fig. 2 as a bar graph.

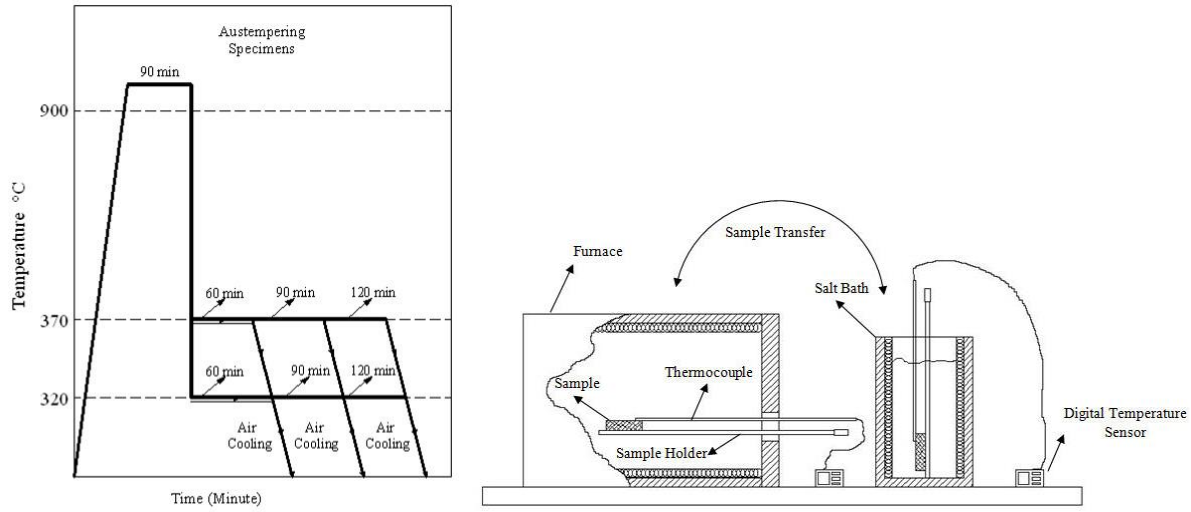

a b

Fig. 1 a - Process of the heat treatment of material; b - experimental set up

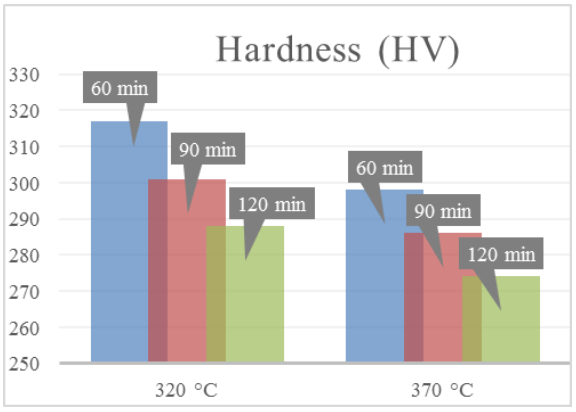

Fig. 2 Hardness values of VGCI under different austempering times and temperatures

Machinability tests were carried on according to ISO 3685. The tests were made at the Johnford TC35 CNC turning center with no cooling liquid at four different cutting speeds (150, 170, 190, 210 m/min), three different feed rates (0.20, 0.25 and 0.30 mm/rev), and a constant cutting depth (2 mm).

Cutting force was measured with a Kistler 9257A three component piezoelectric dynamometer and 5019 B130 charge amplifiers connected to a PC with a Kistler Dynoware force measurement software program. Measurements were made during the machining of the work piece specimens with a length of 20 mm length and a diameter of 26 mm.

2.2. Artificial neural network

Artificial neural network (ANN) system has been designed and developed by modeling the human brain theory. In the brain theory, the synapses collect signals (information), and then transmit them to nuclei (neuron) by means of dendrites. Afterwards, the neuron encodes the signals, and then yields adaptive interactions with the environment [15]. ANNs are a logic programming technique developed with the purpose of automatically performing skills, such as learning, remembering, deciding, and inference, which are features of the human brain, without receiving any aid [16]. The general structure of ANN is given in Fig. 3.

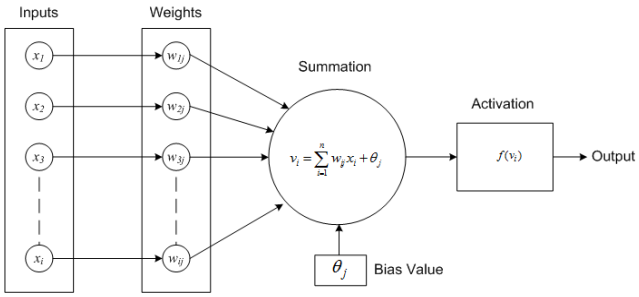

Fig. 3 The structure of ANN

Where, $f(v_i)$ is the activation function, v_i is the weighted sum of the input to the ith processing element, w_{ij} is the weight of the connections between ith and jth processing elements, x_i is the output of the jth processing element, and θ_{ij} is the weights of the biases between layers. Eq. 1 represents the value of the output neuron.

$$v_i = \sum_{i=1}^{n} w_{ij} x_i + \theta_j \ . \tag{1}$$

The activation function provides a curvilinear match between the input and output layers. In addition, it determines the output of the cell by processing the net input to the cell. There are many ways to define the activation function, such as the threshold function, step activa-

tion function, sigmoid function, and hyperbolic tangent function [16]. Hyperbolic tangent transfer function of the ANN model in this study is given in Eq. 2.

$$f(v_i) = \frac{e^{v_i} - e^{-v_i}}{e^{v_i} - e^{-v_i}}. \quad (2)$$

The goal in ANN is to minimize the error value. The weight values are updated until the error falls below the specified value or the number of the maximum loop. Various algorithms and methods are available for the update. In this study, the back propagation algorithm is used to update all weight and bias values depending on the error. The mathematical formulation of the update is given in Eq. 3.

$$w_{ji}^{(l)}(n+1) = w_{ji}^{(l)}(n) + \alpha\left[w_{ji}^{(l)}(n-1)\right] + \\ +\eta\delta_j^{(l)}(n)\, y_i^{(l-1)}(n). \quad (3)$$

Here l is the number of layer, η term is used for the learning coefficient, and δ term is used for the local gradient. They were added to decrease the convergence speed in the decreasing slope method. One of the biggest disadvantages of the back propagation algorithm is the slow convergence feature [17]. This disadvantage is eliminated with the addition of a momentum term (α), as shown in Eq. 3. Momentum training is carried out by retaining the previous values of the weight by adding a memory term into the standard gradient algorithm. Momentum training makes the convergence more stable by increasing the speed. In addition, it prevents the network from sticking to the local minimum [18].

In this study, the learning of ANN was accomplished by a back-propagation algorithm. Back propagation is the most commonly used supervised training algorithm in multilayer feed-forward networks. In back propagation networks, information is processed in the forward direction from the input layer to the hidden layer(s), and then to the output layer. An ANN with a back propagation algorithm learns by changing the connection weights, and these changes are stored as knowledge [19].

2.3. User Interface for ANN

The user interface for ANN training and test steps was developed using Visual C#.Net 2010 (Fig. 4). ANN parameters as number of inputs, outputs, hidden layers, iterations and training data, and momentum and learning rates could be set at the first column. The ANN stop criterion in the second group has two options: the minimum root mean squared error (RMSE) and the number of iterations. While the program is running, the user observes the total RMSE and the number of iterations in the "Current Parameters" group.

After setting the parameters, the "Read Inputs" button must be clicked. It loads the training data set to the table (datagridview) at the right side. After the data are loaded, the prepare button will be visible, and then the start button will appear.

Clicking the start button starts iterations for the learning process. The bias and weight values could be observed in the table at the right side. When the iterations reached the maximum number of iteration or the minimum error, the loop stops and the message appears "the loop stopped because the minimum error was reached".

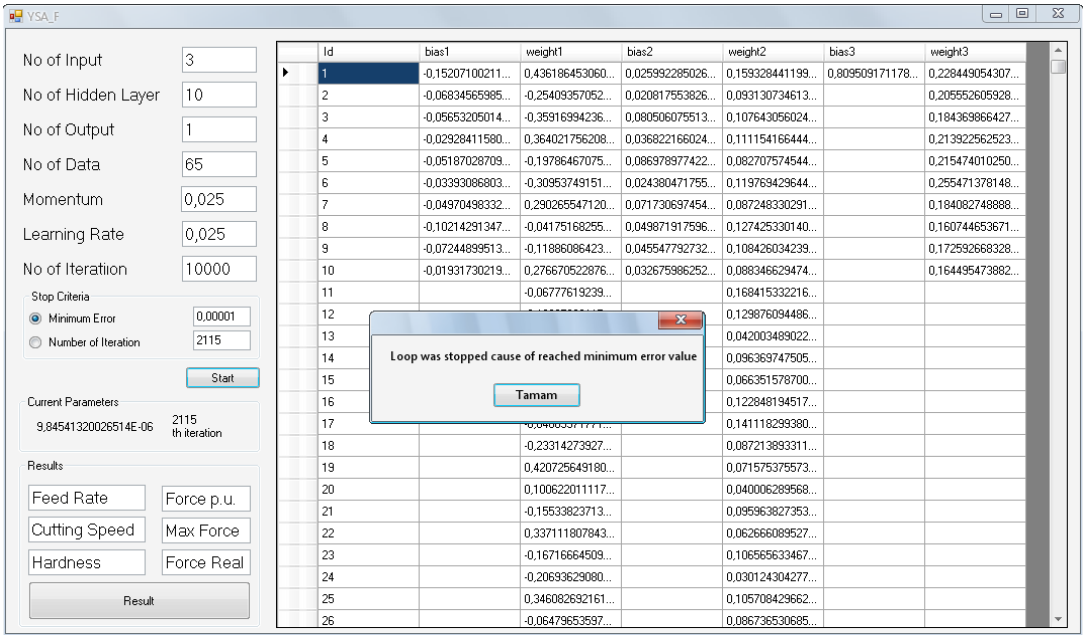

Fig. 4 The view of the user interface when the stop criterion was reached

3. Application of ANN

The ANN model is illustrated in Fig. 5. The values were trained by ANN in two hidden layers in this study. Different network structures were performed and optimized. Best values were kept by 3-12-12-1 network structures with three inputs, one output, and twelve hidden neurons. The input parameters of ANN were hardness, feed rate, and cutting speed. Cutting force values experimentally obtained from a piezoelectric dynamometer constituted the output parameter of ANN.

The experimental design and setup were demonstrated to develop an ANN model real-time cutting force prediction system. In this paper, cutting force was meas-

ured during the turning process of VGCI. The effects of cutting parameters, such as hardness of VGCI, speed and feed rate, were evaluated. The model was formulated for all cutting parameters and machining variables using the neural networks. Then the models were compared for their prediction capability with the actual values. The ANNs are used widely in decision making of complex manufacturing processes, and recently they have been gaining popularity as prediction models.

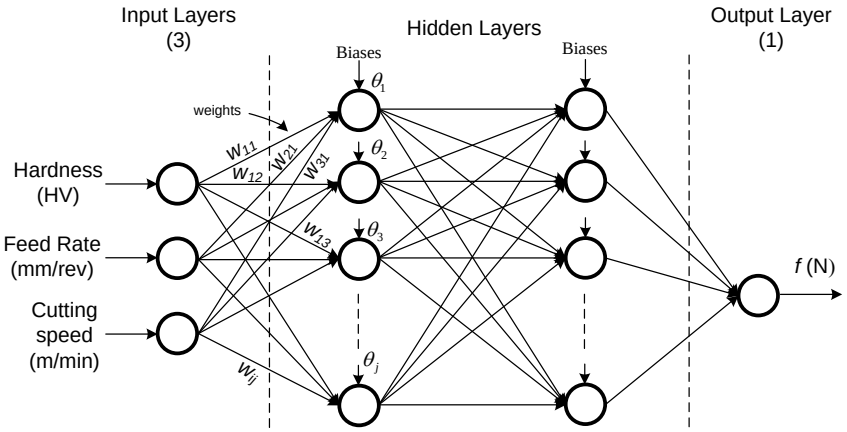

Fig. 5 The ANN structure for application

In this study, 72 experimental data sets were prepared for the training and testing data for the ANN. The ratio for training and testing data was selected as 90:10, i.e. 7 and 65 sets of the experimental data were randomly selected for the testing data and training data, respectively. In the back propagation model, the scaling of inputs and outputs dramatically affects the performance of an ANN [16]. As mentioned above, the logistic hyperbolic tangent transfer function was used in this study. One of the characteristics of this function is that only a value between 0 and 1 can be produced. The input and output data sets were normalized before the training and testing process to obtain the optimal predictions. Hardness, feed rate, cutting speed, and cutting force were normalized by dividing by 317, 0.3, 210, and 788.71, respectively.

Cutting force values predicted after ANN training were compared with values obtained from the experimental study. Predictive accuracy was evaluated using the root mean squared error (*RMSE*), coefficient determination (R^2), mean absolute error (*MAE*), and mean percentage error (*MPE*).

RMSE provides information on the short term efficiency, which is a benchmark of the differences between the predicted and observed values. Also, this value was used in ANN to stop the learning process. The lower the *RMSE*, the more accurate is the evaluation and coefficient of determination (also called *R* square), which measures the variance that is interpreted by the model, which is the reduction of variance. R^2 orders from 0 to 1 while the model has healthy predictive ability when it is near to 1. These performance metrics are good measures of the overall predictive accuracy. MAE (mean absolute error) is an indication of the average deviation of the predicted values from the corresponding observed values and can present information on the long term performance of the models. The lower the *MAE*, the better the long term model prediction is. The Mean Percentage Error (*MPE*) is a well-known measure that corrects the 'cancelling out' results and also keeps into basis the different scales at which this measure can be calculated and thus can be used to analyze different predictions [20, 21].

The error calculation formulas are represented in Eqs. (4)-(7).

$$RMSE = \sqrt{\frac{1}{n}\sum_{k=1}^{n}\left|y_k - \hat{y}_k\right|^2}\ ; \tag{4}$$

$$MAE = \frac{1}{n}\sum_{k=1}^{n}\left|y_k - \hat{y}_k\right|\ ; \tag{5}$$

$$MPE = \frac{1}{n}\sum_{k=1}^{n}\frac{y_k - \hat{y}_k}{\hat{y}_k} * 100\ ; \tag{6}$$

$$R^2 = 1 - \left(\frac{\sum_{k=1}^{n}\left|y_k - \hat{y}_k\right|^2}{\sum_{k=1}^{n}\hat{y}_k{}^2}\right). \tag{7}$$

4. Results and discussion

The predictive accuracy of a neural network model was evaluated through coefficient determination via *RMSE*, R^2, *MAE*, and *MPE*. *RMSE* and R^2 provide baseline measures of predictive accuracy. All results reported are for the training set and test set. The predictive estimation results are summarized in Table 2.

The ANN results showed that the predictive values were very close to the real values. *RMSE* and R^2 normalized test results were 0.0163 and 0.9962, respectively.

The graphs of the regression analysis for both normalized and real data pertaining to the training and test values are given in Figs. 6 and 7. Training data results were very close to the real numbers. The predicted values were around the trend line.

The comparison graph of the measured and predicted results for the normalized and real training data are given in Fig. 8. The fluctuations in the graph are very similar and they almost overlap. In Fig. 9, the graphs represent normalized and real test data results of ANN. The differences between measured and predicted *F* values for 7 test data were in an acceptable range.

Table 2

Accuracy of predictions of the neural network model

	RMSE		***R^2***		***MAE***		***MPE***	
	Training	**Test**	**Training**	**Test**	**Training**	**Test**	**Training**	**Test**
Normalized	1.16E-07	0.0163	0.9999	0.9962	8.25E-08	0.0046	9.73E-06	0.5530
Real	9.12E-05	12.8452	0.9999	0.9962	6.50E-05	3.6000	9.73E-06	0.5530

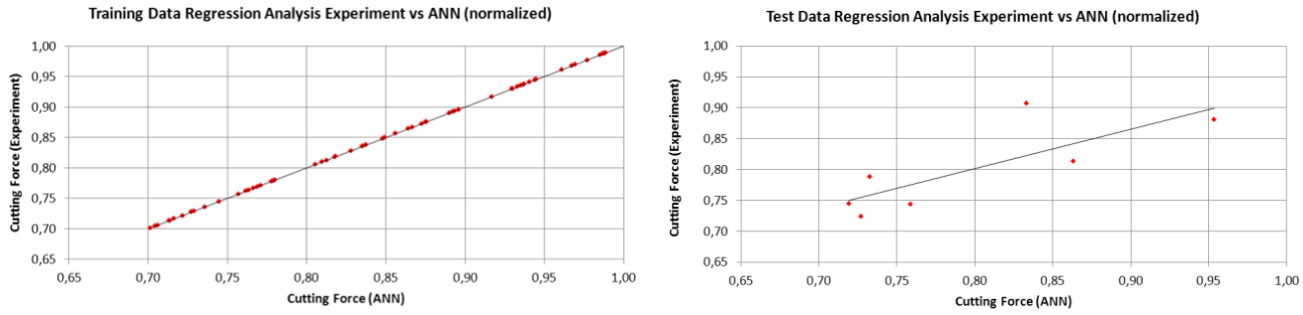

a b

Fig. 6 Cutting force normalized data regression analysis: a - training; b - test

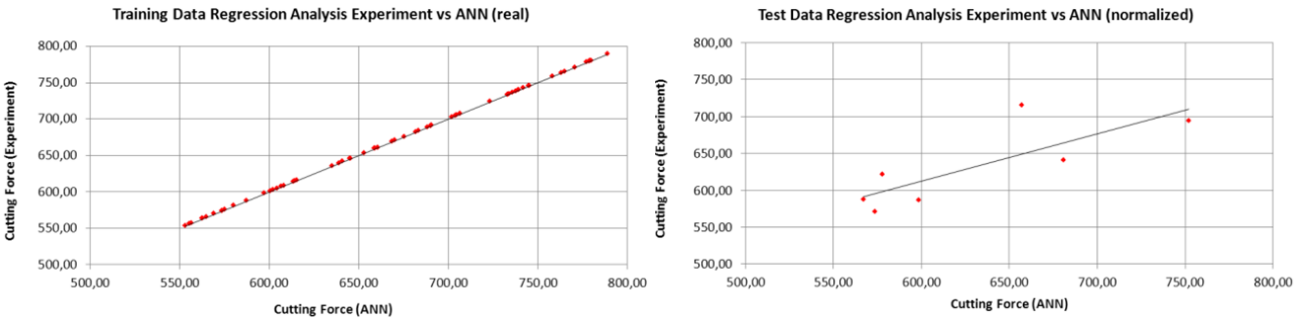

a b

Fig. 7 Cutting force real data regression analysis: a - training; b - test

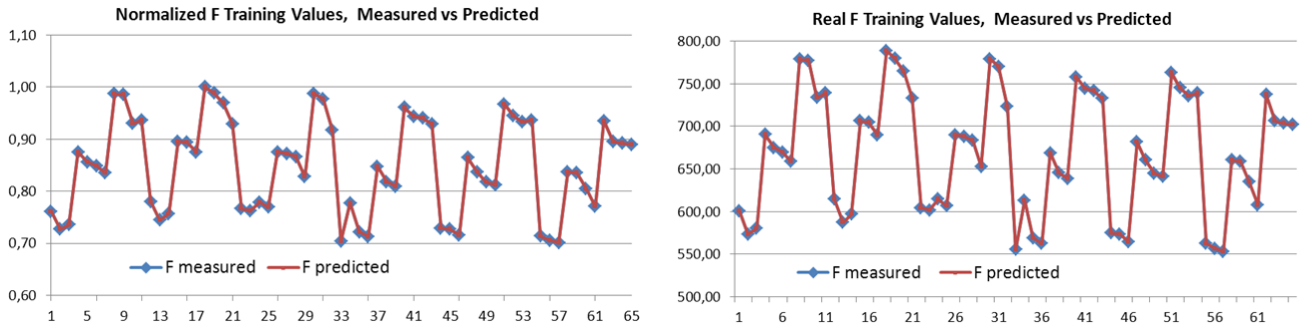

a b

Fig. 8 Comparison between measured and ANN training output values: a - normalized; b - real

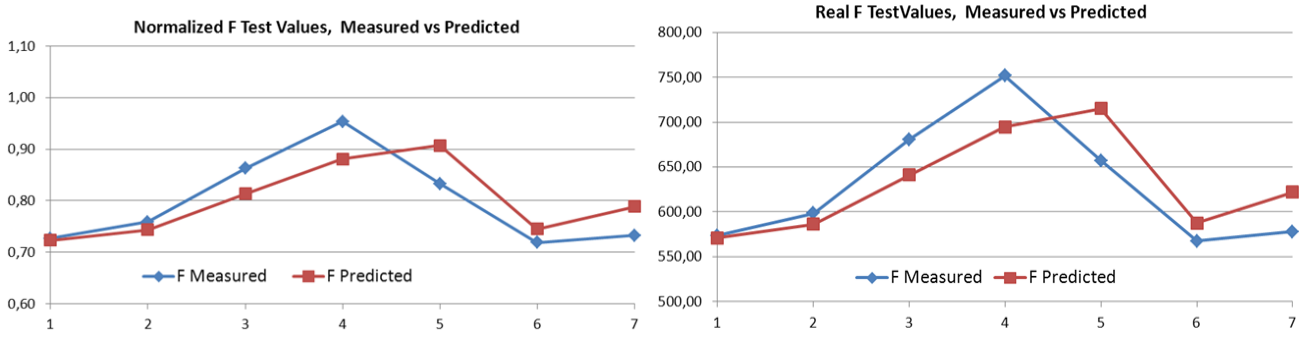

a b

Fig. 9 Comparison between measured and ANN test output values: a - normalized; b - real

5. Conclusions

In the present work, experimental and modeling studies show that the cutting force of austempered vermicular graphite cast irons can be controlled with austempering heat treatment and machining parameters. Artificial neural networks can be used for the prediction of the cutting force. The results can be summarized in the experimental section results and modeling section results. Feed possesses the most significant effect on cutting force followed by cutting speed. An increment of cutting speed and decrement of feed result in better cutting forces.

In the design of the proposed model, hardness, feed rate, and cutting speed were selected as input parameters of the artificial neural network. The best network structure with minimum error rate was achieved by 3-12-12-1. The ANN model, developed to predict the cutting force value, provided predicted values very close to the actual values found in the experiments. The predictive accuracy of the neural network model evaluated via RMSE, R^2, MAE, and MPE. The R^2 results of ANN were 99.99% and 99.62% for training and test values, respectively, which were very high.

Acknowledgement

The authors would like to acknowledge Gazi University Scientific Research Project (07/2011-14) for the financial support throughout this study.

References

1. **Akkurt, M.** 1992. Talaş Kaldırma Yöntemleri ve Takım Tezgahları. Birsen Yayınevi, Istanbul.
2. **Stafanescu, D.M.** 1999. Classification and Basic Metallurgy of Cast Iron. ASM Handbook, USA.
3. **Walton, C.F.** 1991. Introduction to the Heat Treating of Cast Irons, ASM International, USA.
4. **Elliot, R.** 1988. Cast Iron Technology, Butterworths&Co., London, 252 p.
5. **Elliott, R.** 2006. Cast Irons. Wiley-VCH Verlag GmbH & Co. KGaA.
6. **Putatunda, S.K.** 2001. Development of austempered ductile cast iron (ADI) with simultaneous high yield strength and fracture toughness by a novel two-step austempering process, Materials Science and Engineering a-Structural Materials Properties Microstructure and Processing 315(1-2): 70-80. http://dx.doi.org/10.1016/S0921-5093(01)01210-2.
7. **Seker, U.; Hasirci, H.** 2006. Evaluation of machinability of austempered ductile irons in terms of cutting forces and surface quality, Journal of Materials Processing Technology 173(3): 260-268. http://dx.doi.org/10.1016/j.jmatprotec.2005.05.058.
8. **Cakir, M.C.; Bayram, A.; Isik, Y.; Salar, B.** 2005. The effects of austempering temperature and time onto the machinability of austempered ductile iron, Materials Science and Engineering a-Structural Materials Properties Microstructure and Processing 407(1-2): 147-153. http://dx.doi.org/10.1016/j.msea.2005.07.005.
9. **Hanafi, I.; Khamlichi, A.; Cabrera, F. M.; Lopez, P. J. N.; Jabbouri, A.** 2012. Fuzzy rule based predictive model for cutting force in turning of reinforced PEEK composite, Measurement 45(6): 1424-1435. http://dx.doi.org/10.1016/j.measurement.2012.03.022.
10. **Jinsheng, W.; Gong, Y.; Shi, J.; Abba, G.** 2009. Surface roughness prediction in micromilling using neural networks and Taguchi's design of experiments, IEEE International Conference on Industrial Technology, Australia, 10-13 Feb.
11. **Bartarya, G.; Choudhury, S.K.** 2012. Effect of cutting parameters on cutting force and surface roughness during finish hard turning AISI52100 grade steel, Fifth Cirp Conference on High Performance Cutting 2012, 1: 651-656. http://dx.doi.org/10.1016/j.procir.2012.04.116.
12. **Aouici, H.; Yallese, M.A.; Chaoui, K.; Mabrouki, T.; Rigal, J.-F.** 2012. Analysis of surface roughness and cutting force components in hard turning with CBN tool: Prediction model and cutting conditions optimization, Measurement 45(3): 344-353. http://dx.doi.org/10.1016/j.measurement.2011.11.011.
13. **Irgolic, T.; Franc, C.; Matej, P.; Joze, B.** 2014. Prediction of cutting forces with neural network by milling functionally graded material, Procedia Engineering 69: 804-813. http://dx.doi.org/10.1016/j.proeng.2014.03.057.
14. **Selvaraj, D.P.; Chandramohan, P.; Mohanraj, M.** 2014. Optimization of surface roughness, cutting force and tool wear of nitrogen alloyed duplex stainless steel in a dry turning process using Taguchi method, Measurement 49: 205-215. http://dx.doi.org/10.1016/j.measurement.2013.11.037.
15. **Arbib, M.A.** 2002. The Handbook of Brain Theory and Neural Networks. London: MIT Press, 1344 p.
16. **Cay, Y.; Korkmaz, I.; Cicek, A.; Kara, F.** 2013. Prediction of engine performance and exhaust emissions for gasoline and methanol using artificial neural network, Energy 50: 177-186. http://dx.doi.org/10.1016/j.energy.2012.10.052.
17. **Dursun, M.; Ozden, S.** 2014. An efficient improved photovoltaic irrigation system with artificial neural network based modeling of soil moisture distribution - A case study in Turkey, Computers and Electronics in Agriculture 102: 120-126. http://dx.doi.org/10.1016/j.compag.2014.01.008.
18. **Dursun, M.; Karaman, M.R.** 2009. Artificial neural network based modeling of spatial distribution of phosphorus on the tomato area, Asian Journal of Chemistry 21(1): 239-247.
19. **Xie, H.; Ma, F.; Bai, Q. 2009.** Prediction of indoor air quality using artificial neural networks, Fifth International Conference on Natural Computation, 414-418, China. http://dx.doi.org/10.1109/icnc.2009.502.
20. **Doreswamy, V.; Chanabasayya, M.** 2013. Performance analysis of neural network models for oxazolines and oxazoles derivatives descriptor dataset, International Journal of Information Sciences and Techniques (IJIST) 3(6): 1-15.
21. **Maran, J.P.; Sivakumar, V.; Thirugnanasambandham, K.; Sridhar, R.** 2013. Artificial neural network and response surface methodology modeling in mass transfer parameters predictions during osmotic dehydration of Carica papaya L, Alexandria Engineering Journal 52: 507-516. http://dx.doi.org/10.1016/j.aej.2013.06.007.

Ahmet Mavi, Semih Ozden, İhsan Korkut

PREDICTION AND EXPERIMENTAL STUDY ON CUTTING FORCE OF AUSTEMPERED VERMICULAR GRAPHITE CAST IRON USING ARTIFICIAL NEURAL NETWORK

S u m m a r y

In this study, a technique was proposed to predict cutting force of austempered vermicular graphite cast irons (VGCI) by using neural network. The effect of austempering heat treatment on the cutting force was experimentally achieved. The samples were austenitized at 900°C for 90 minutes and then austempered at different temperatures (320°C and 370°C) for 60, 90, and 120 minutes. Machinability tests were carried out under dry conditions at the CNC machining center with the cutting parameters selected in accordance with ISO 3685. In the experiment, cutting force depending on hardness, cutting speed, and feed rate were measured. These results were used for input parameters (training, testing, and validation) of Artificial Neural Network (ANN) and prediction model was developed. The output value of ANN and experimental results were compared and accuracy of ANN was found to be 99.99% and 99.62% for training and test values, respectively.

Keywords: artificial neural network, cutting force, machining, vermicular graphite cast iron, heat treatment.

Received November 24, 2015
Accepted February 06, 2017